

Supporting Information

Dual-channel fluorescent probe bearing two-photon activity for cell viability monitoring

Yanqian Zhao^{a†}, Chengkai Zhang^{a†}, Jiejie Liu^{b†}, Dandan Li^{*a}, Aidong Wang^c,
Xiaohe Tian^b, Shengli Li^a, Jieying Wu^a, Yupeng Tian^{*a}

^aCollege of Chemistry and Chemical Engineering, Institutes of Physics Science and Information Technology, Key Laboratory of Functional Inorganic Materials Chemistry of Anhui Province, Anhui Province Key Laboratory of Chemistry for Inorganic/Organic Hybrid Functionalized Materials, Anhui University, Hefei 230601, People's Republic of China.

^bSchool of Life Science, Anhui University, Hefei 230601, P. R. China.

^cSchool of Chemistry and Chemical Engineering, Huangshan College, Huangshan University, Huangshan 245041, P. R. China.

[†]These authors contributed equally to this work.

*Corresponding author: chemlidd@163.com; yptian@ahu.edu.cn

Experimental Section	3
1.1 Materials and Apparatus.....	3
1.2 Computational details	3
1.3. Two-photon excited fluorescence (TPEF) spectroscopy.....	3
1.4 Cytotoxicity assays in cells	4
1.5 Cell culture and staining	4
1.6 DNase and RNase treatment	5
1.7 Molecular docking with RNA/DNA	5
1.8 Synthesis	6
Scheme S1 The synthetic procedures of dyes 1OC and 2OC	6
Results and discussions.....	8
(1) Mechanism of avoiding aggregation-induced quenching.....	8
(2) Validation of specific bind with RNA	8
Fig. S3 ^1H -NMR spectrum of 2OC.....	10
Fig. S4 ^{13}C -NMR spectrum of 2OC.....	10
Fig. S8 Absorption spectra (left) and plot (right) of intensity against the concentration of (a) 1OC, (c) 2OC respectively in H_2O buffered with HEPES.....	13
Fig. S11 Models obtained by molecular modeling for the interaction of 2OC with RNA fragment.	14
Fig. S12 (a) SPEF changes of 10 μM 2OC with 200 μM DNA. (b) Models obtained by molecular modeling for the interaction of 2OC with DNA fragment.	15
Fig. S13 Deoxyribonuclease (DNase) and ribonuclease (RNase) digest experiments of 2OC ($\lambda_{\text{ex}} = 550$ nm) using single-photon fluorescent images.....	15
References.....	15

Experimental Section

1.1 Materials and Apparatus

All chemicals and solvents were dried and purified by usual methods. The synthetic routes for the compounds and their derivatives were illustrated in **Scheme. S1**. Both the compounds were purified over recrystallization. The ^1H -NMR and ^{13}C -NMR spectra recorded on at 25°C, using Bruker 400/600 Ultrashield spectrometer were reported as parts per million (ppm) from TMS (δ). ESI Mass Spectrometer was recorded using LCQ Fleet. UV-vis absorption spectra were recorded on a UV-265 spectrophotometer. Fluorescence measurements were carried out on a Hitachi F-7000 fluorescence spectrophotometer.

1.2 Computational details

To better understand the charge transfer state, time-dependent density functional theory (TD-DFT) calculations on all the compounds were carried out in THF. Optimizations were carried out with B3LYP functional without any symmetry restraint, and the TD-DFT calculations were performed on the optimized structure with B3LYP functional. All calculations, including optimizations and TD-DFT, were performed with the G09 software. Geometry optimization of the singlet ground state and the TD-DFT calculation of the lowest 25 singlet–singlet excitation energies were calculated with a basis set composed of 6-31 G* for C H N O S P F atoms. An analytical frequency confirms evidence that the calculated species represents a true minimum without imaginary frequencies on the respective potential energy surface. The lowest 25 spin-allowed singlet-singlet transitions, up to energy of about 5 eV, were taken into account in the calculation of the absorption spectra.

1.3. Two-photon excited fluorescence (TPEF) spectroscopy

Two-photon cross-sections of the compounds were recorded using two-photon excited fluorescence measurements with a femtosecond laser pulse, to avoid the possibility of excited state absorption, and a Ti: sapphire system (690-1080 nm, 80 MHz, 140 fs) as the light source. The 2PA cross section (σ) was determined by comparing their TPEF to that of fluorescein, according to the following equation:

$$\sigma_s = \frac{\sigma_r \times F_s \times C_r \times n_r}{F_r \times \Phi_s \times C_s \times n_s}$$

where the subscripts “s” and “r” represent sample and reference (here, Rhodamine B in ethanol solution was used as reference and samples were all in concentration of 1.0×10^{-5} mol/L with a 1 cm standard quartz cell). F is the two-photon excited fluorescence integral intensity of the solution emitted at the exciting wavelength. F, n and c are the quantum yield of the fluorescence, the refractive index of the solvent, and the concentration of the solution, respectively. The values of “s” and “r” at different wavelengths and Fr are taken from the literature.

1.4 Cytotoxicity assays in cells

The study of the effect of **1OC** and **2OC** on viability of cells was carried out using the methylthiazolylidiphenyl-tetrazolium bromide (MTT) assay. Hela cells were cultured in a 96-well plate for 24h before experiments. The cell medium was then exchanged by different concentrations of **1OC** and **2OC** medium solutions (5, 10, 15, 20, 25 μ M). They were then incubated at 37 °C in 5 % CO₂ for 24 h before cell viability was measured by the MTT assay. The cell medium solutions were exchanged by 100 μ L of fresh medium, followed by the addition of 20 μ L (5 mg/mL) MTT solution to each well. The cell plates were then incubated at 37 °C in 5 % CO₂ for 4 h. Absorbance was measured at 570 nm. The absorbance measured for an untreated cell population under the same experimental conditions was used as the reference point to establish 100% cell viability. Duplicated experiments have been tested.

1.5 Cell culture and staining

For confocal microscopy, cells were imaged on a ZEISS LSM 710 META confocal laser-scanning microscope with a 63x and 100x oil lens. Image data acquisition and processing was performed using Zeiss LSM Image Browser, Zeiss LSM Image Expert and Image J. For real-time live cell imaging, the incubation chamber was connected to a ZEISS temperature control unit at 37 °C and a CO₂ controller with appropriate humidity. For transmission electron microscopy (TEM), cell samples were received pelleted in Eppendorf tubes. HeLa cells were incubated with complex **1OC** and **2OC** (30 min) and then fixed in 3 % glutaraldehyde and

dehydrated in ethanol. The sections were examined using a FEI Tecnai Transmission Electron Microscope at an accelerating voltage of 80 kV. Electron micrographs were taken using a Gatan digital camera.

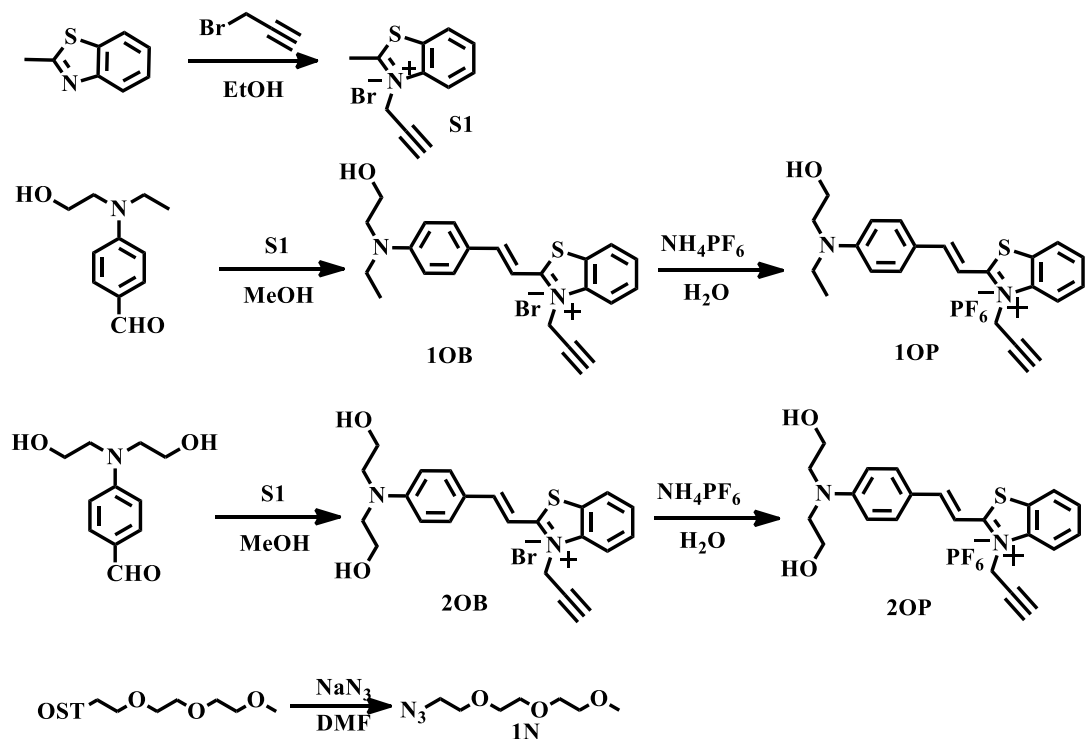
1.6 DNase and RNase treatment

For DNase and RNase digest test, two sets of living Hela cells were stained with 15 μ M **2OC** in PBS (pH = 7.4) for 30 min. After washing with PBS twice, a total 1mL PBS (as control experiment) was added into a set of cells and 25 mg/mL DNase-Free RNase or RNase-Free DNase was added into the other set of cells, and then two sets of cells were incubated at 37 °C in 5 % CO₂ for 2 h. In addition, the DNase and RNase digest tests of cells stained with 30 μ M **2OC** was also carried out for comparison.

1.7 Molecular docking with RNA/DNA

Molecular docking techniques are valuable tools in understanding the nature of RNA/DNA interaction for the molecule design and the mechanistic study, **Fig. 7d** and **Fig. S11-S12**. The molecular interactions of **2OC** with RNA/DNA are obtained through the LigandFit docking method. LigandFit docking is based on an initial shape match to the binding site, through a variety of scoring functions (PMF, PLP and LigScore), to obtain the comprehensive docking score, and further get the highest score as well as the best docking model. On the basis of the data obtained by the above methods, we conducted molecular modelling calculations using Discovery Studio 4.16 with the double stranded RNA/DNA fragment and single stranded RNA/DNA fragment.

1.8 Synthesis



Scheme S1 The synthetic procedures of dyes **1OC** and **2OC**.

Synthesis of S1: 3-bromopropylene (7.02 g, 0.06 mol) and methylbenzothiazole (8.94 g, 0.06 mol) was dissolved in 20 mL acetonitrile, heated reflux 4 h. Then the solution cool to room temperature, filtered, washed with ether, vacuum dry, we obtain white solid 15 g, the yield 94 %. $^1\text{H-NMR}$ (d_6 -DMSO, 400 MHz, ppm) δ 8.52 (d, J = 7.9 Hz, 1H), 8.38 (d, J = 8.5 Hz 1H), 7.94 (m, 1H), 7.84 (dd, J = 11.4 Hz, 3.9 Hz, 1H), 5.79 (d, J = 2.5 Hz, 2H), 3.84 (s, 1H), 3.29 (s, 3H). $^{13}\text{C-NMR}$ (d_6 -DMSO, 100 MHz, ppm) δ 178.49, 140.24, 129.56, 129.00, 128.30, 124.92, 116.70, 79.01, 74.61, 17.19. ESI-MS (m/z) Calcd. for $\text{C}_{11}\text{H}_{10}\text{NS}^+$: 188.05, Found: 188.05.

Synthesis of 1N: NaN_3 (0.51 g, 7.85 mmol) was added TsO_3 (1.0 g, 3.14 mmol) and DMF (125 mL) with stirring 24 h at room temperature in 250 mL round bottom flask. And the solution used water to quench reaction, extracted by dichloromethane, turned out dichloromethane, dried in the vacuum drying oven, finally obtaining the product 1.2 g, the yield 82 %. $^1\text{H NMR}$ (d_6 -Acetone, 400 MHz, ppm) δ 3.70 (m, 2H), 3.59 (d, J = 10.0, 6.4 Hz, 6H), 3.51 (m, 2H), 3.42 (m, 2H), 3.29 (s, 3H). $^{13}\text{C NMR}$ (d_6 -Acetone, 100 MHz, ppm) δ 72.68, 71.31, 71.24, 71.15, 70.75, 58.85,

51.41.ESI-MS (*m/z*) Calcd. for [C₇H₁₅N₃O₃+H]⁺: 189.05; Found: 189.05.

Synthesis of 1OP: 10 mL methanol as solvent, and 2 drops of piperidine as catalyst was added into 50 mL round bottom flask with 4-[(2-azethylethyl)(ethyl) amino) benzaldehyde (0.96 g, 5 mmol) and **S1** (1.34 g, 5 mmol), refluxed 12 h. Then, in 25 mL beaker dissolve 1.84 g (10 mmol) NH₄PF₆ with 15 mL absolute acetonitrile, and add the solution to the round bottom flask. Stirring, up to 45 °C return 1 h. Cool, slowly add a small amount of acetone, filtered, wash with anhydrous ether several times, 2 g purple solid obtained, yield 94 %. ¹H-NMR (*d*₆-DMSO, 400 MHz, ppm) δ 8.27 (d, *J* = 8.0 Hz, 1H), 8.11 (s, 1H), 8.08 (d, *J* = 7.3 Hz, 1H), 7.88 (d, *J* = 8.7 Hz, 2H), 7.79 (t, *J* = 7.8 Hz, 1H), 7.68 (d, *J* = 7.9 Hz, 1H), 7.63 (m, 1H), 6.87 (d, *J* = 8.9 Hz, 2H), 5.76 (s, 2H), 3.73 (s, 1H), 3.64 (t, *J* = 5.8 Hz, 3H), 3.68 (m, 4H), 1.17 (t, *J* = 6.9 Hz, 3H). ¹³C NMR (*d*₆-DMSO, 100 MHz, ppm) δ 171.09, 152.61, 151.44, 140.34, 133.62, 128.96, 127.40, 126.50, 123.95, 121.20, 115.42, 112.05, 104.61, 78.05, 76.04, 58.45, 52.06, 45.29, 37.41, 11.99. ESI-MS (*m/z*) Calcd for C₂₂H₂₃N₂OS⁺: 363.15; Found: 363.15.

Synthesis of 2OP: The synthesis of 2OP is the same as that of 1OP synthesis. ¹H-NMR (*d*₆-DMSO, 400 MHz, ppm) δ 8.31 (d, *J* = 7.8 Hz, 1H), 8.14 (d, *J* = 8.6 Hz, 1H), 8.11 (s, 1H), 7.90 (d, *J* = 8.8 Hz, 2H), 7.80 (t, *J* = 7.4 Hz, 1H), 7.70 (s, 1H), 7.67 (d, *J* = 7.9 Hz, 1H), 6.93 (d, *J* = 9.0 Hz, 2H), 5.78 (d, *J* = 1.8 Hz, 2H), 4.90 (s, 2H), 3.73 (s, 1H), 3.63 (s, 8H). ¹³C-NMR (*d*₆-DMSO, 100 MHz, ppm) δ 171.22, 153.10, 151.45, 140.39, 133.52, 126.56, 124.06, 121.36, 115.51, 112.28, 104.87, 78.08, 76.07, 58.17, 53.16. Anal. Calc. for C₂₂H₂₃F₆N₂O₂PS (%): C, 50.38; H, 4.42; N, 5.34. Found: C, 50.38; H, 4.42; N, 5.35. ESI-MS (*m/z*) Calcd. for C₂₂H₂₃N₂O₂S⁺: 379.14; Found: 379.14.

1OC: 1OP (0.51 g, 1 mmol) and **1N** (0.19 g, 1 mmol) was added into the 50 mL round bottom flagon 10 mL of methanol and acetonitrile as solvent, continue to add 6 drops DIPEA and 0.2 g CuI as the catalyst, and reflux overnight. The organic solvent was removed on a rotary evaporator resulting. Column chromatography separate products and impurities (Ethyl acetate: methanol = 5:1). 0.51 g purple solid obtained, the yield was 87 %.

2OC: the synthetic route of compound **2OC** is similar to that of **1OC**. Characterization data can be found in supporting information.

Results and discussions

(1) Mechanism of avoiding aggregation-induced quenching

To verify that **1OC** and **2OC** do not undergo aggregative fluorescence quenching in a biological environment, fluorescence emission spectra of **1OC** and **2OC** were measured at 350 nm at room temperature as shown in Fig. S7. It is clear that **1OC** and **2OC** showed two emission bands at 400 nm and 600 nm, where both emission intensities were found to be enhanced by increasing proportions of glycerol in the mixture solvent. Due to the presence of trans double bonds in **1OC** and **2OC**, different rigid aromatic ring groups rotate around the double bond connected to the core, which causes the excited state energy to be dissipated, resulting in quenching of the fluorescence emission;¹ Molecular torsion was inhibited by increasing glycerol ratio. Energy consumption is reduced, leading to fluorescence enhancement. Therefore, **1OC** and **2OC** can suppressed aggregation-induced quenching.²

(2) Validation of specific bind with RNA

To further confirm whether **2OC** is selective for DNA or RNA, we performed using deoxyribonuclease (DNase) and ribonuclease (RNase),³ as shown in Fig. S13. RNase is a special enzyme that hydrolyzes RNA without interfering with DNA, and DNase hydrolyzes DNA without interfering with RNA.⁴ After RNase digestion, the single photon fluorescence signal of **2OC** in the nucleolus was significantly weaker than that of the undigested sample. After DNase digestion, the single photon fluorescence signal of **2OC** in the nucleolus still exists. These results show that **2OC** can specifically stain RNA in nucleolus.

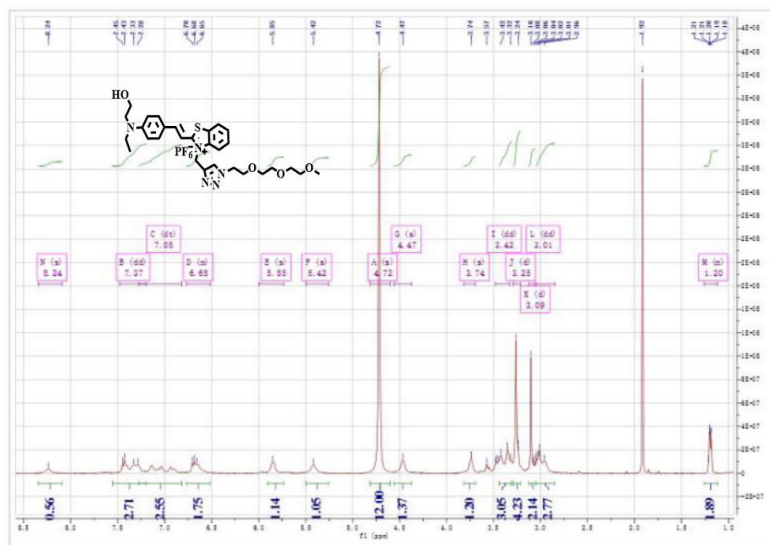


Fig. S1 ¹H-NMR spectrum of **1OC**.

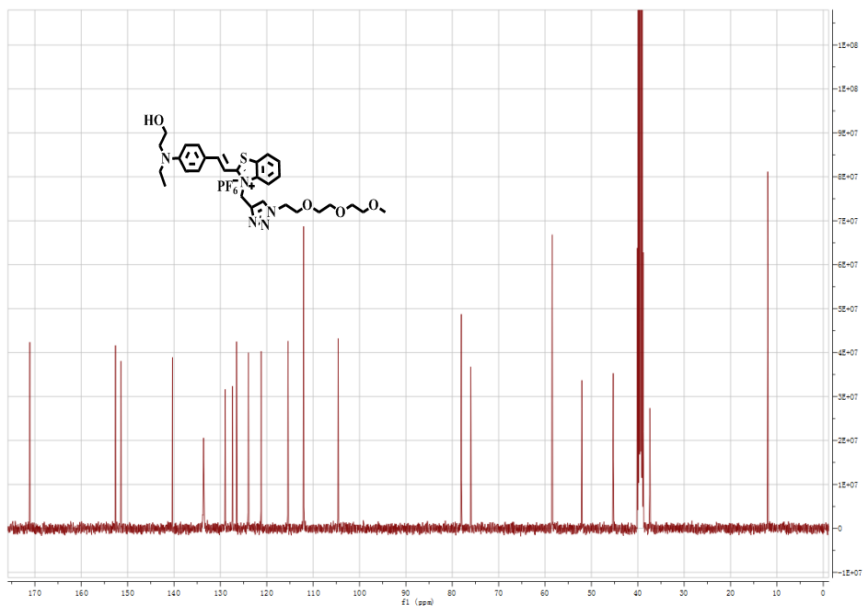


Fig. S2 ¹³C-NMR spectrum of **1OC**.

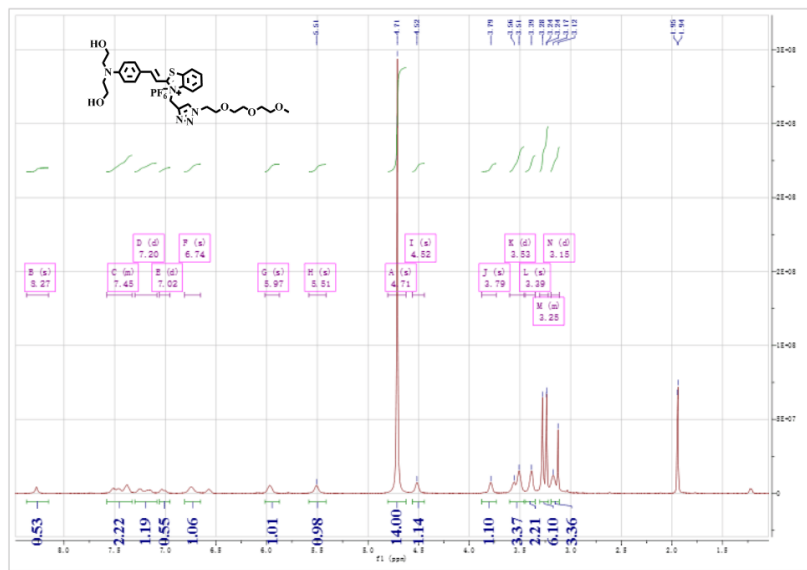


Fig. S3 ^1H -NMR spectrum of **2OC**.

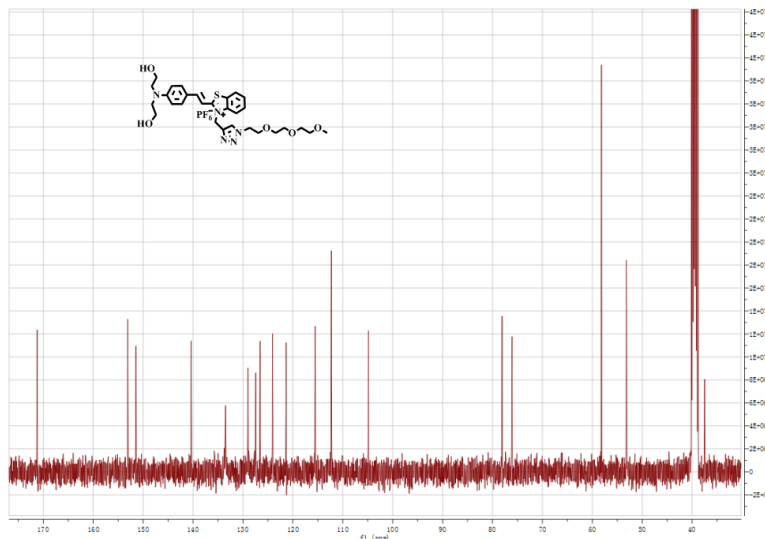


Fig. S4 ^{13}C -NMR spectrum of **2OC**.

Table S1 Fluorescence quantum yield of **2OC** at 500 and 625 nm.

2OC	500 nm	625 nm
	1.94 %	6.74 %

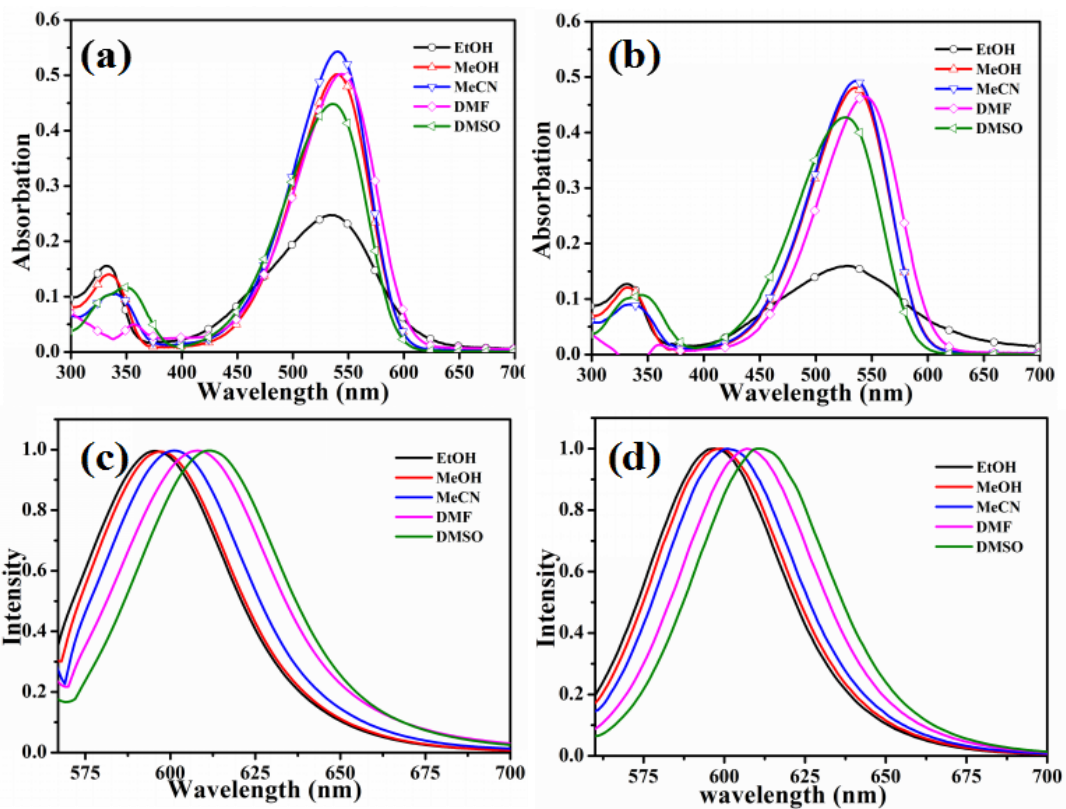


Fig. S5 Uv-vis absorption and fluorescence spectra of **1OC** and **2OC** in different solvents.

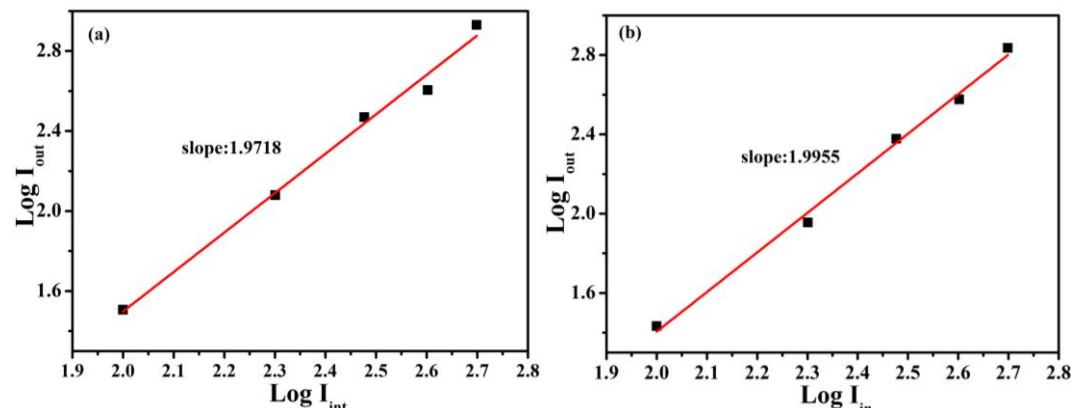


Fig. S6 Output fluorescence (I_{out}) vs. the square of input laser power (I_{in}) for **1OC**, **2OC** in DMSO.

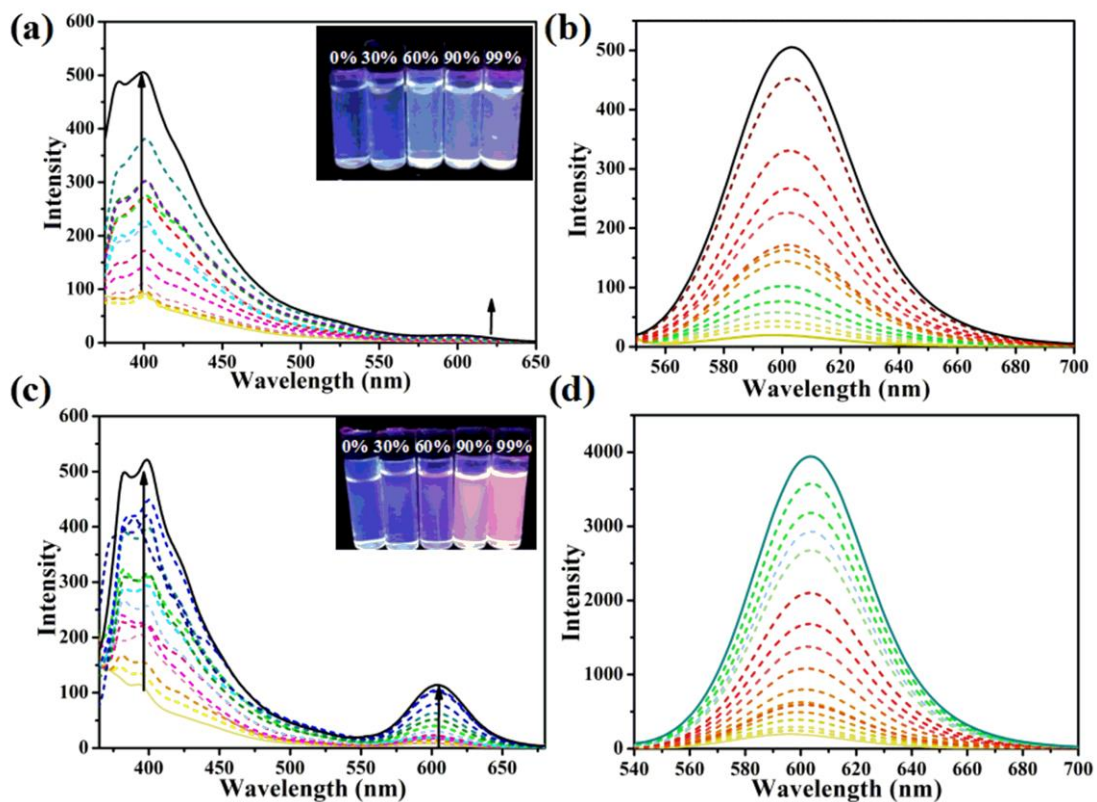


Fig. S7 Changes of **1OC** and **2OC** fluorescence spectra with the variation of solution viscosity in a water-glycerol system , (a) $\lambda^{1OC}_{ex} = 345$ nm. (b) $\lambda^{1OC}_{ex} = 526$ nm. (c) $\lambda^{2OC}_{ex} = 359$ nm. (d) $\lambda^{2OC}_{ex} = 536$ nm. Inset in (a) and (c), fluorescence changes of **1OC** and **2OC** in 0.00 % to 99 % glycerol system glycerol system under UV light (365 nm excitation).

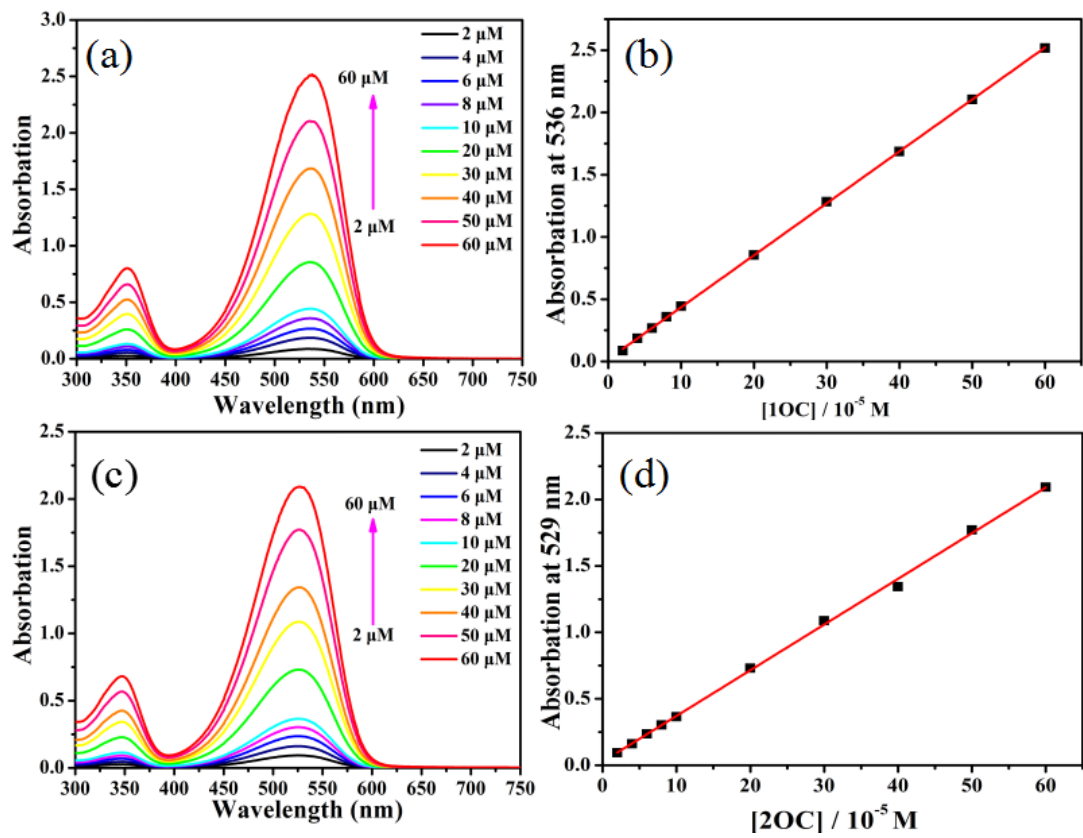


Fig. S8 Absorption spectra (left) and plot (right) of intensity against the concentration of (a) **1OC**, (c) **2OC** respectively in H₂O buffered with HEPES.

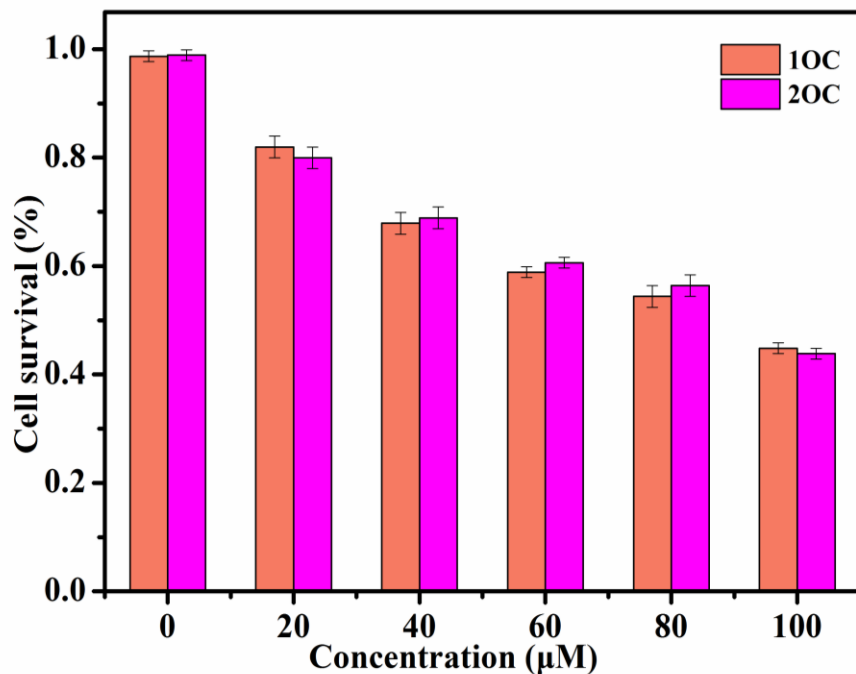


Fig. S9 Cytotoxicity data results of **1OC** and **2OC** at different concentrations for 24 h.

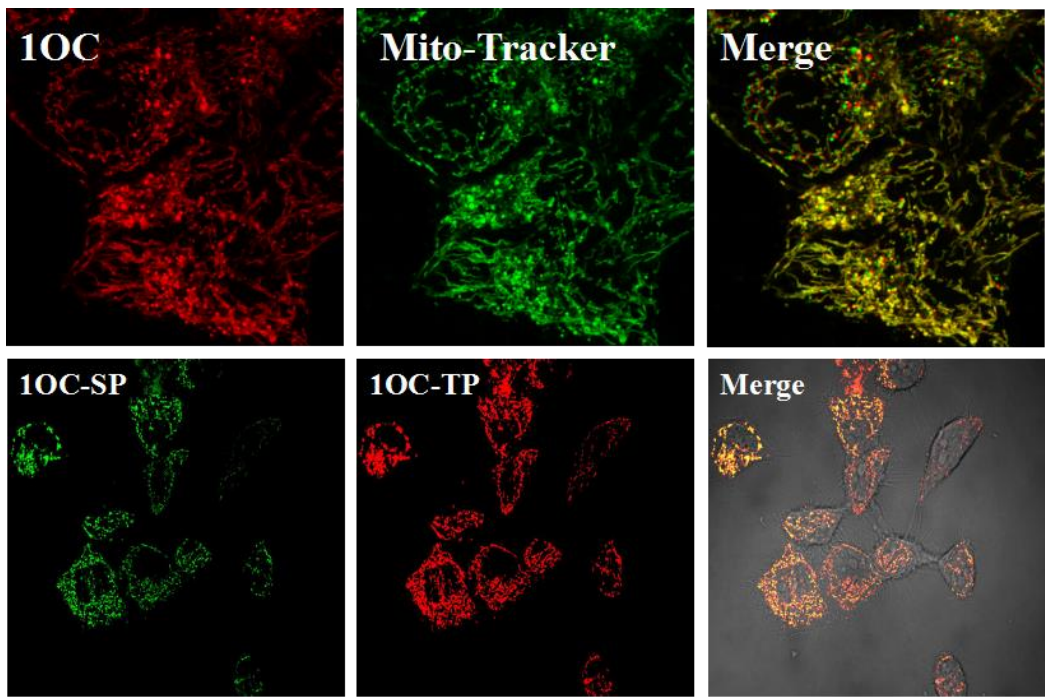


Fig. S10 Confocal fluorescence images of **1OC** in HeLa cells. Single-photon imaging (green, $\lambda_{\text{ex}} = 405$ nm), two-photon imaging (red, $\lambda_{\text{ex}} = 900$ nm), and merge image.

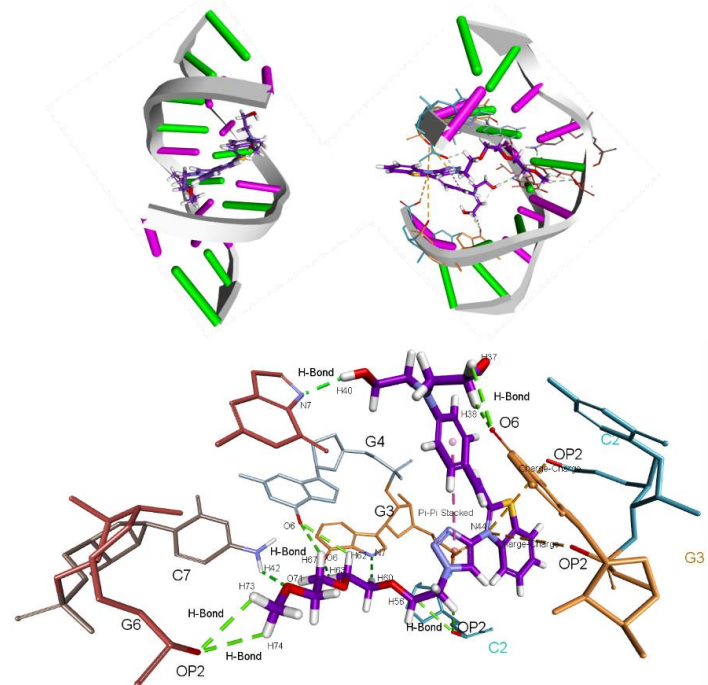


Fig. S11 Models obtained by molecular modeling for the interaction of **2OC** with RNA fragment.

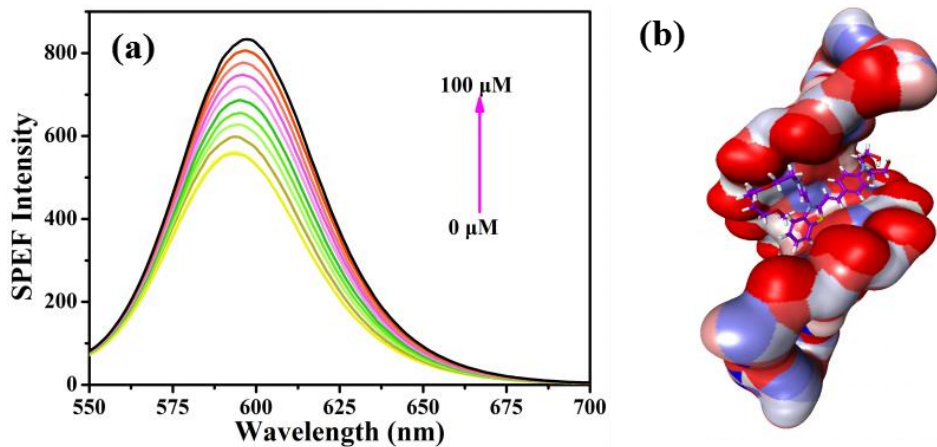


Fig. S12 (a) SPEF changes of 10 μM **2OC** with 200 μM DNA. (b) Models obtained by molecular modeling for the interaction of **2OC** with DNA fragment.

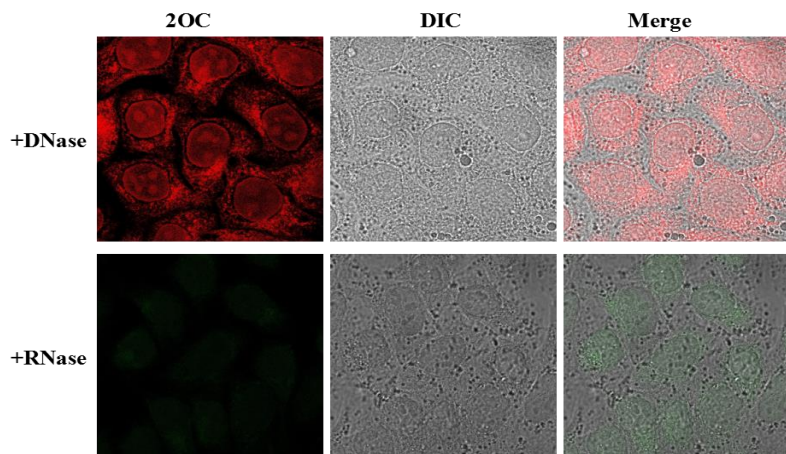


Fig. S13 Deoxyribonuclease (DNase) and ribonuclease (RNase) digest experiments of **2OC** ($\lambda_{\text{ex}} = 550$ nm) using single-photon fluorescent images.

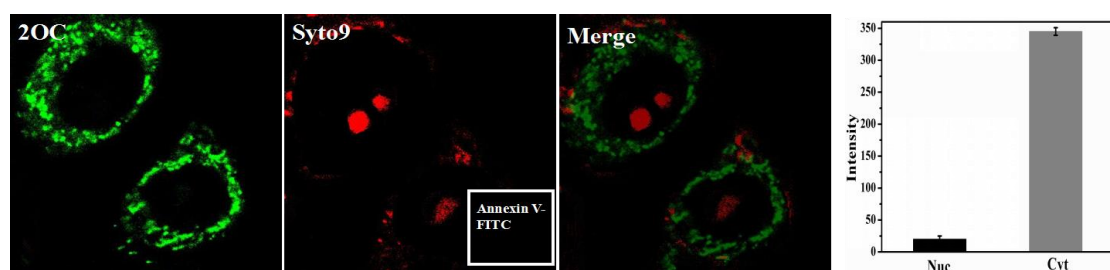


Fig. S14 Live cell stain with **2OC** (10 μM) and co-stain with Syto9/Annexin V-FITC. Relative fluorescence intensity of Cyt (cytoplasmic) and Nuc (nuclear) in HeLa cells.

References

1. F. Liu, T. Wu, J. Cao, S. Cui, Z. Yang, X. Qiang, S. Sun, F. Song, J. Fan, J. Wang and X. Peng, *Chem. Eur. J.*, 2013, **19**, 1548.
2. Y. Hong, J. W. Y. Lamab and B. Z. Tang, *Chem. Soc. Rev.*, 2011, **40**, 5361.

3. K.-N. Wang, X.-J. Chao, B. Liu, D.-J. Zhou, L. He, X.-H. Zheng, Q. Cao, C.-P. Tan, C. Zhang and Z.-W. Mao, *Chem. Commun.*, 2018, **54**, 2635.
4. W. Du, H. Wang, Y. Zhu, X. Tian, M. Zhang, Q. Zhang, S. C. D. Souza, A. Wang, H. Zhou, Z. Zhang, J. Wu and Y. Tian, *ACS Appl. Mater. Interfaces*, 2017, **9**, 31424.